BOREAL ENVIRONMENT RESEARCH 21: 221–229
ISSN 1239-6095 (print) ISSN 1797-2469 (online)

Helsinki 23 May 2016

Electric wind in a Differential Mobility Analyzer

Maris Palo[1)], Meelis Eller[1)], Janek Uin[2)] and Eduard Tamm[1)]

[1)] *Laboratory of Environmental Physics, Institute of Physics, University of Tartu, Ülikooli 18, EE-50090 Tartu, Estonia*
[2)] *Biological, Environmental & Climate Sciences Department, Brookhaven National Laboratory, Upton, NY 11973-5000, USA*

Received 14 July 2015, final version received 24 Oct. 2015, accepted 25 Oct. 2015

Palo M., Eller M., Uin J. & Tamm E. 2016: Electric wind in a Differential Mobility Analyzer. *Boreal Env. Res.* 21: 221–229.

Electric wind — the movement of gas, induced by ions moving in an electric field — can be a distorting factor in size distribution measurements using Differential Mobility Analyzers (DMAs). The aim of this study was to determine the conditions under which electric wind occurs in the locally-built VLDMA (Very Long Differential Mobility Analyzer) and TSI Long-DMA (3081) and to describe the associated distortion of the measured spectra. Electric wind proved to be promoted by the increase of electric field strength, aerosol layer thickness, particle number concentration and particle size. The measured size spectra revealed three types of distortion: widening of the size distribution, shift of the mode of the distribution to smaller diameters and smoothing out the peaks of the multiply charged particles. Electric wind may therefore be a source of severe distortion of the spectrum when measuring large particles at high concentrations.

Introduction

Atmospheric aerosols substantially affect climate, air quality and human health (Hinds 1999, Chow *et al*. 2006, Seinfeld and Pandis 2006). Therefore great effort has been made to develop methods to accurately describe the properties of atmospheric aerosol. Since the effects of the aerosol particles are mostly dependent on their size, atmospheric aerosol is well characterized by the size distribution of the particles (Hinds 1999). Particle size can be measured using various methods, among which the electrical separation method (Liu and Pui 1974) is one of the most common and simplest. This method is used by the Differential Mobility Analyzer (DMA) (Knutson and Whitby 1975, Hoppel 1978, Flagan 1998) that separates particles according to their electrical mobility and determines the mobility spectrum, from which a size spectrum can be determined. For faster measurements Wang and Flagan (1990) developed the scanning DMA technique that was further incorporated into TSI's Scanning Mobility Particle Sizer (SMPS).

The size spectrum measured by the DMA can however be distorted by a number of factors like airflow turbulence, decentralization of electrodes, etc. A study by Peil and Tamm (1984) showed that measurements could also be disturbed by electrostatic destabilization of the laminar flow in the DMA. Occurrence of such disturbance was confirmed by Uin *et al*. (2011). Ku *et al*. (2006) considered the same phenomenon to be the cause of anomalous responses observed in a DMA when characterizing aggregates of

Editor in charge of this article: Veli-Matti Kerminen

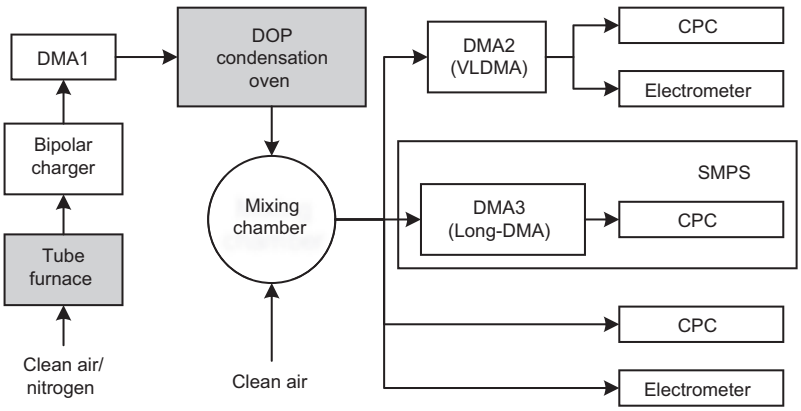

Fig. 1. Experimental setup for particle generation and measurements. For generating multiply charged particles, DMA1 was not used and the sequence of the charger and the DOP oven were switched.

airborne carbon nanotubes or nanofibers. This phenomenon can be called electric wind (also ionic wind, corona wind or electrohydrodynamic thrust) although, as explained below, in this case this term is not strictly correct.

The electric wind is the movement of gas, induced by (light or cluster) ions moving in an electric field (Harney 1957, Robinson 1960, Robinson 1962, Hawley 1965). It is a characteristic feature of corona discharge that was first observed during the electrostatic studies at the beginning of the 18th century, and was a subject of active investigation during the 18th and 19th centuries (Robinson 1962). In the case of corona discharge, the momentum of ions gained from the electric field is passed onto the surrounding gas molecules upon elastic impacts creating pressure differences between microscopic volumes of gas and produces a turbulent flow of gas (Hawley 1965).

In a DMA, the main movement is the laminar flow of the aerosol and sheath air in the axial direction. The additional turbulent air movement is induced not by cluster ions but by charged aerosol particles, which unlike cluster ions being objects of microscopic world are objects of macroscopic world. However, as the physical mechanisms of these two phenomena are very similar, the term "electric wind" is used below. Although up to now most of the DMA users did not considered such an effect in the DMA, the electric wind always causes turbulence and must therefore be avoided in aerosol particle mobility measurements.

So far, the occurrence of the electric wind in a DMA has not been thoroughly investigated. The aim of this study was to experimentally determine the conditions under which electric wind occurs in the locally-built VLDMA (Very Long Differential Mobility Analyzer) (Uin and Tamm 2010) and TSI Long-DMA (3081), and to describe the associated distortion of the measured spectrum.

Methods

Particle generation and measurements

Aerosol particles were generated using the scheme (Fig. 1) previously described by Uin and Tamm (2010) and Uin *et al*. (2009). A condensation generator (tube furnace) was used to generate silver particles in the 2–40 nm diameter range. Pressurized clean air or nitrogen was used as the carrier gas. The particles were charged using a ^{239}Pu bipolar diffusion charger. An overwhelming majority of these small particles remain uncharged or acquire only one elementary charge in a bipolar ionic field (Fuchs 1963, Wiedensohler 1988). For further investigation, only negatively charged particles were selected by a DMA (DMA1 in Fig. 1) to avoid coagulation of particles with opposite charge polarities. The charged particles were then grown in a condensation oven by the condensation of dioctyl phthalate (DOP) vapor and transported to a mixing chamber where particle-free dilution air was added. It is important to note, that the grown (large) particles remain singly charged (Uin *et al*. 2009). Varying the temperature of the DOP generator and the amount of dilution air allowed

selecting the mean particle size and concentration of particles, accordingly. The particles were classified using a Long-DMA (DMA3 in Fig. 1) or the VLDMA (DMA2 in Fig. 1). The ratio of aerosol flow to DMA sheath air flow was varied to change the thickness of the particle cloud inside the DMA. The number concentration of the particles was measured with a TSI 3776 CPC or a Faraday cup aerosol electrometer. For some experiments multiply charged particles were generated using an alternative generation scheme (Uin *et al*. 2009) where the particles are grown before charging and are therefore more likely to obtain charge larger than $\pm 1e$ (they obtain stationary charge distribution characteristic for their mean diameter). With this scheme DMA1 was not used and the places of the condensation oven and the diffusion charger were switched (Fig. 1).

Unlike the well-known TSI Long-DMA, the locally-built VLDMA is only briefly described in the two papers mentioned above. Therefore, it is useful to present some main parameters of the instrument: diameters of the inner and outer electrodes are 84.3 and 100.0 mm, accordingly; the active length (distance between input and output slits) is 1200 mm. For this study different aerosol and sheath air flow rates Q_a and Q_{sh} were used retaining Q_a/Q_{sh} ratio of 1:10 or 1:5; Reynolds number for the flow in the channel with annular cross-section between cylindrical electrodes was in the range from 20 to 140.

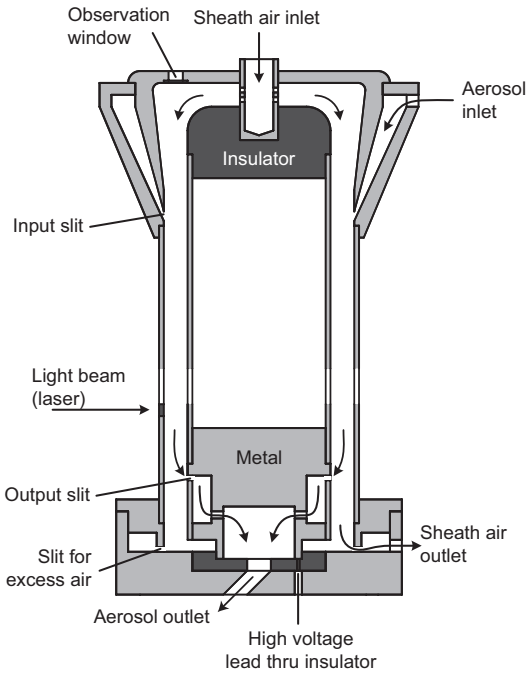

Fig. 2. Schematic diagram of the locally-built VLDMA, showing the two windows for electric wind investigations.

Visual detection of the electric wind

The VLDMA is equipped with two windows: one on the side, near the exit slit for a laser beam to illuminate the inside of the DMA, and the other on top for visual observations (Fig. 2). The occurrence and the threshold conditions of electric wind can be assessed from the changes in the light pattern seen through the observation window. When no electric wind occurs, the light pattern is stable, reflections of the electrodes and a narrow aerosol layer between them can be seen (Fig. 3a). When intensive electric wind occurs, the aerosol layer changes and turbulent movements can be seen as waves and eddies (Fig. 3b).

The visual detection experiments investigated the effects of electric field strength, the mean particle size, the total particle concentration and particle layer thickness inside the DMA on the formation of electric wind. A threshold electric field strength value was found by changing the voltage applied to the DMA electrodes and determining the conditions close to the onset of electric wind: increasing the voltage evokes and intensifies waves while decreasing the voltage makes the particle layer more stable. If the formation of the electric wind is not promoted under the chosen conditions, more momentum from the electric field is needed for electric wind to develop and higher threshold electric field strength is observed.

This method is not exact, since determining the threshold value depends on the intensity of the scattered light and the results are influenced by the subjective judgment of the observers, especially at low particle number concentrations. The effects of observer subjectivity were minimized by repeating the experiments and having at least three persons make the observations.

A special question can arise about the effect of the non-conductive and plane (not cylindrical) glass surface of the lower window on the flow

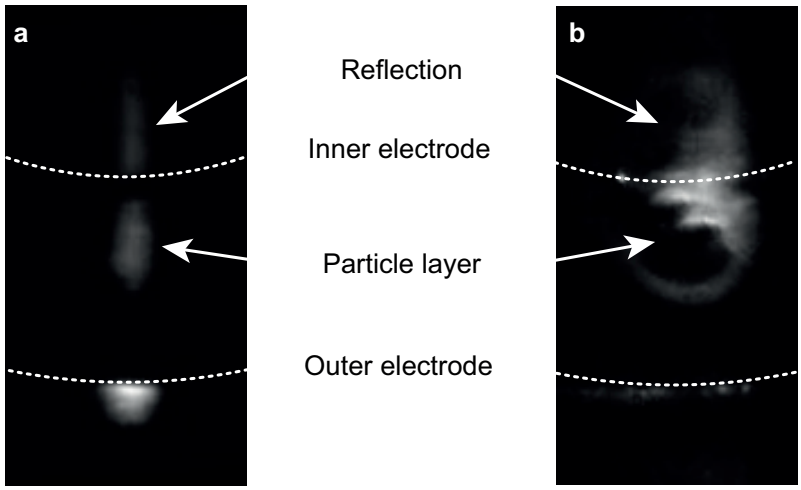

Fig. 3. The light pattern seen through the VLDMA observation window (**a**) when no electric wind occurs, and (**b**) with intensive electric wind. Particles with the mean particle diameter 1740 nm and total particle number concentration of 1×10^7 cm^{-3} at Q_{sh} = 10 l min^{-1} and Q_a = 1 l min^{-1} were studied at electric field strengths of (**a**) 110 kV m^{-1} and (**b**) 382 kV m^{-1}. In panel **b**, the aerosol layer is very close to the inner electrode due to higher field strength and the light scattered by the particle layer coincides with its reflection from inner electrode. Dashed lines are added to indicate the locations of the electrodes.

and electric field near the window. Diameter of the glass window is 9 mm. Absence of the flow distortion was checked by switching off the electric field: we see the undistorted aerosol layer in the vicinity of the outer electrode. Local distortion of the electric field cannot be the substantial reason for the electric wind, as in the light scattered by the particles, eddies and waves of the aerosol layer are clearly seen in the neighborhood of the directly illuminated area.

Distortions of the measured size distribution associated with electric wind

When measuring the particle size spectrum, the voltage applied to the DMA electrodes is gradually increased and, at any given voltage, only particles with electrical mobility in a narrow range, determined by the DMA transfer function corresponding to that voltage, should be separated out. When electric wind occurs, some particles move in turbulent waves. The particles that reach the output slit may not represent the expected electrical mobility. Therefore, the particle number concentration can be either over- or underestimated. This can cause significant distortions in the measured particle size spectrum. The effect of the chosen experimental conditions on the formation of electric wind can therefore be assessed according to the occurrence and extent of these distortions. The characteristics of the spectra measured with VLDMA and Long-DMA at different total particle concentrations, mean particle diameters and charge distribution were therefore compared. Some changes in the measured size distribution were determined by fitting a lognormal distribution to the measured spectra.

Results and discussion

The experiments demonstrated well the effects of particle number concentration and cloud thickness on the formation of electric wind. The increase of the particle number concentration resulted in the decrease of the electric field strength needed for electric wind to develop (Fig. 4). Plotting the threshold electric field strength against the reciprocal of the particle number concentration yields a linear dependence (i.e. the threshold electric field strength dependence on concentration is hyperbolic). This experimental finding enables to

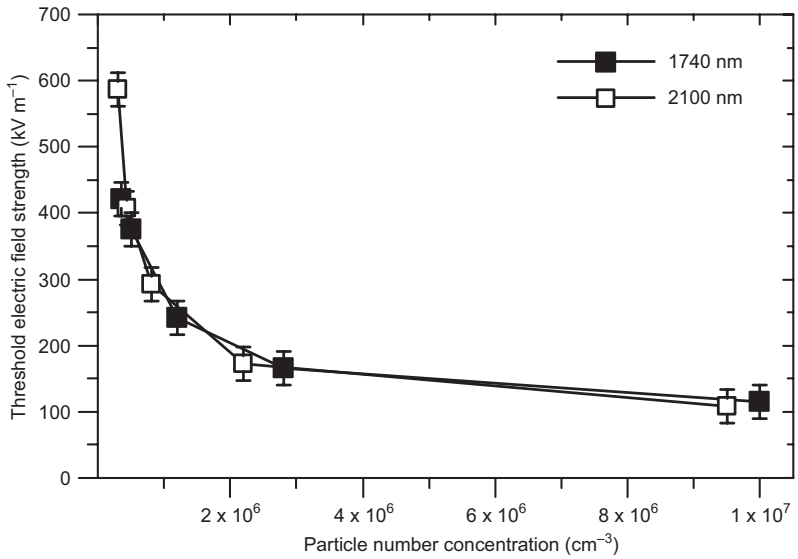

Fig. 4. The threshold electric field strength at different total particle number concentrations in VLDMA. Error bars show the uncertainty of visual detection of the threshold electric field strength.

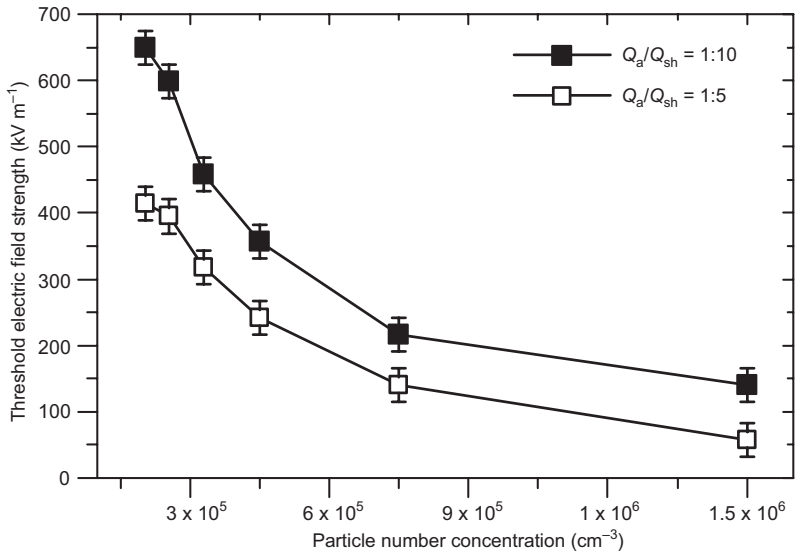

Fig. 5. The threshold electric field strength at different total particle number concentrations in VLDMA at different particle layer thicknesses (determined by ratio of aerosol flow Q_a to sheath air flow Q_{sh}). Mean particle diameter is approximately 2060 nm. Error bars show the uncertainty of visual detection of the threshold electric field strength.

derive a general criterion for the onset of electric wind (electrostatic destabilization of a laminar flow) in a DMA and other similar flow systems. A theoretical discussion on this subject will be presented in a future paper.

In case of a thicker aerosol cloud (changing the ratio of aerosol to sheath air flow from 1:10 to 1:5, layer thickness 0.8 mm and 1.6 mm, respectively), lower electric field strength was needed for the onset of electric wind at the same particle number concentration (Fig. 5).

In all the following figures, with exception of Fig. 9, information about singly-charged particles is presented. For singly-charged particles, the particle diameter and electrical mobility are uniquely related. We, therefore, can study particle size, although the DMA classifies particles according to their electrical mobility.

The investigation of the measured size spectra revealed three main changes associated with electric wind: shifting of the mode of the distribution to smaller diameters, the increase of the width of the size distribution [standard deviation of the fitted lognormal distribution, $\ln(\sigma_g)$] and smoothing out the peaks of multiply charged particles.

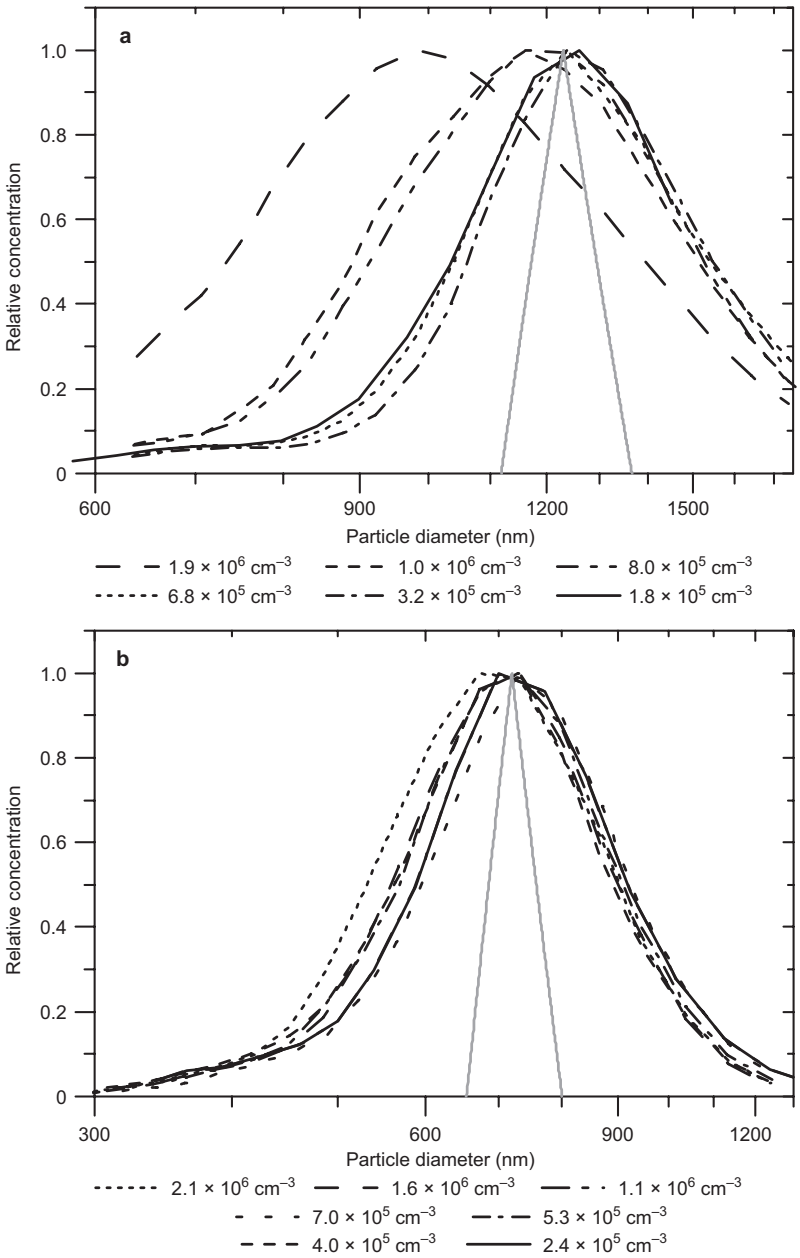

Fig. 6. Particle size distributions as measured by the VLDMA at different total particle number concentrations. Mean particle diameter is approximately (**a**) 1230 nm and (**b**) 720 nm. Relative concentration is normalized to the highest measured concentration. The gray solid line shows the transfer function of the DMA.

The shift of the mode indicates that because of eddies caused by electric wind particles are pulled to the output slit at voltages corresponding to higher electrical mobilities and are therefore interpreted as smaller particles. The turbulent movements also stretch the aerosol layer wider and therefore seemingly increase the width of the measured distribution.

Multiply charged particles have higher electrical mobility than singly charged particles of the same size and are therefore interpreted as smaller particles in the size spectrum measurements using DMAs. This manifests as additional peaks in the measured size distribution at smaller diameters. In case of intensive electric wind the distribution curves of both singly and multiply charged particles are distorted: the mode is shifted to smaller diameters and the distribution width increases. As a result the peaks of multiply charged particles are smoothed out. Adding

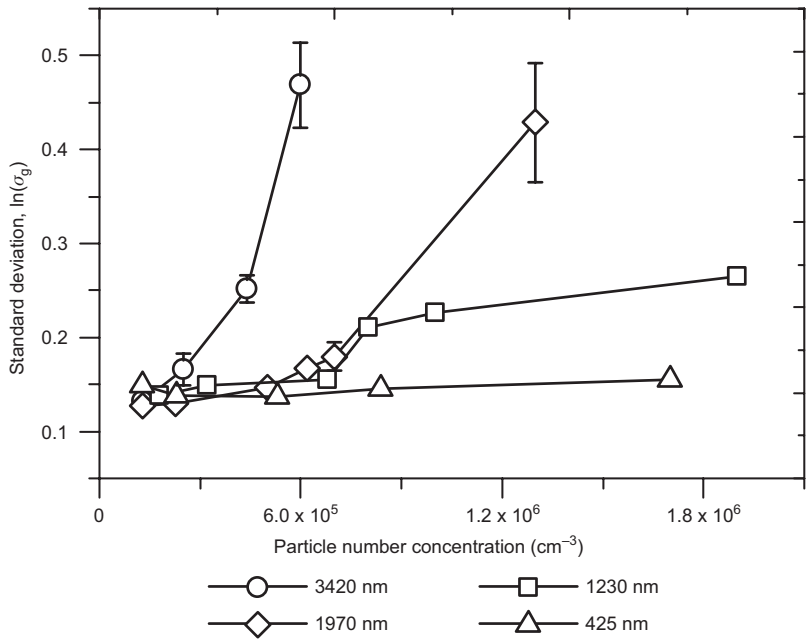

Fig. 7. Width of the particle size distribution measured by the VLDMA [standard deviation of the fitted lognormal distribution, ln(σ_g)] as a function of total particle number concentration. Error bars show the standard error of the distribution width parameter.

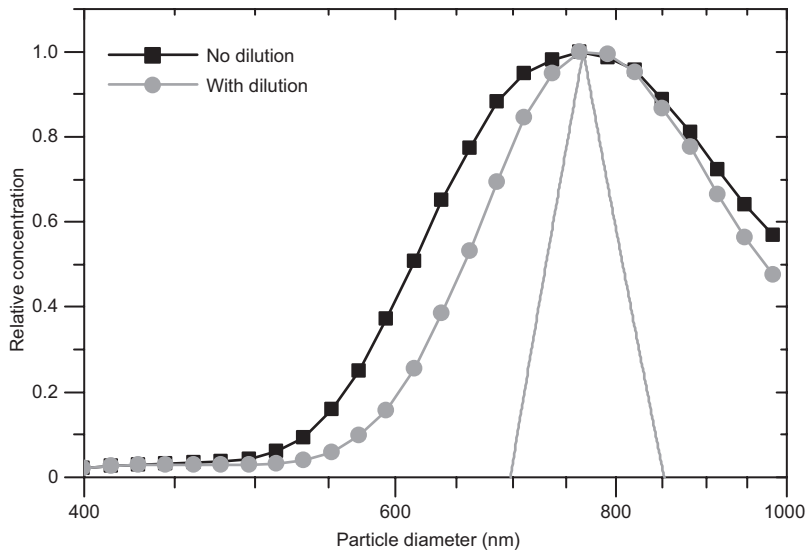

Fig. 8. Particle size distribution as measured by Long-DMA without dilution (total particle number concentration about 6.36 $\times$ 10^6 cm^{-3}) and with about 1:5 dilution. Mean particle diameter is approximately 760 nm. Relative concentration is normalized to the highest measured concentration. The grey solid line shows the transfer function of the DMA.

enough dilution air suppresses the electric wind and the peaks of multiply charged particles become visible again.

The shift of the mode and the increase of the width of the size distribution were seen in the VLDMA size distribution measurement results at different total particle concentrations (Fig. 6a). By comparing Fig. 6a and b we note that the extent of the shift of the mode increases with particle size. Fitting a lognormal distribution to the measured spectra revealed that particle size also promotes the increase of the distribution width (Fig. 7). The experiments with the Long-DMA demonstrated the increase of the standard deviation of the lognormal fit as well (Fig. 8), but the shift of the distribution mode was not clear. The smoothing of the peaks of multiply charged particles generated by the alternative scheme was seen in both, the VLDMA and Long-DMA measurement results. This effect is shown in Fig. 9 for Long-DMA which is a widely used instrument and this knowledge should therefore

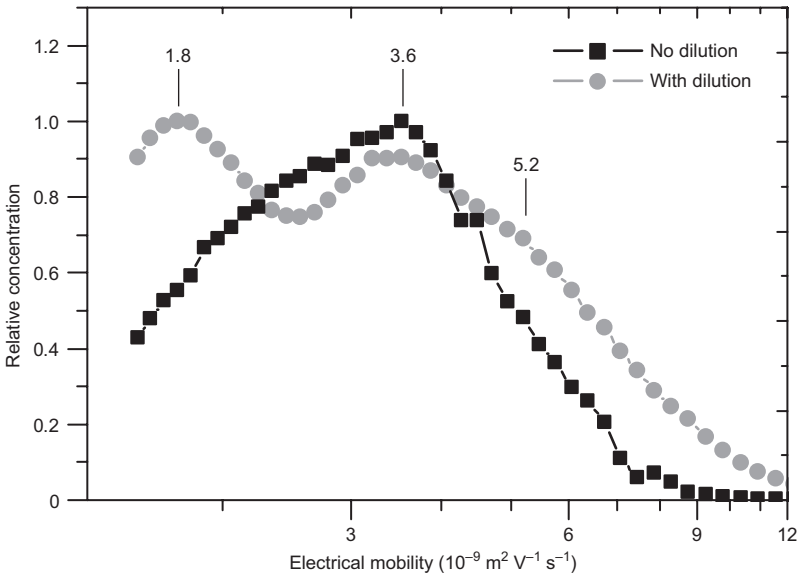

Fig. 9. Electrical mobility distribution of multiply charged particles (generated by the alternative scheme, explained above) as measured by Long-DMA without dilution (total particle number concentration about 2.69×10^7 cm^{-3}) and with about 1:35 dilution. Mean particle diameter is approximately 650 nm (peak of singly-charged particles). The location of the peaks and the corresponding electrical mobility of particles with one, two and three elementary charges are presented in the figure. Relative concentration is normalized to the highest measured concentration.

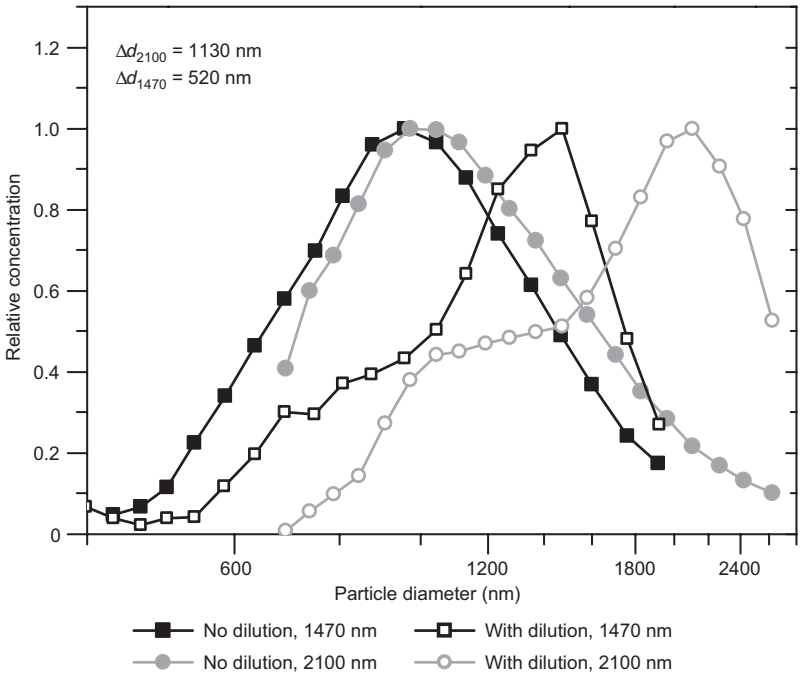

Fig. 10. Size distributions of multiply charged particles (from coagulation of silver particles with the same charge polarity) as measured by the VLDMA without dilution (total particle number concentration about 10^7 cm^{-3}) and with about 1:5 dilution. Mean particle diameters are approximately 1470 nm and 2100 nm. Relative concentration is normalized to the highest measured concentration.

be interesting for many investigators. Peaks of particles with three, four and more elementary charges are in this case smoothed due to the insufficient resolution of the Long-DMA. The shift of the distribution mode and also smoothing out the peaks of multiply charged particles is depicted in Fig. 10. When particle size increases from 1470 nm to 2100 nm, the shift of the distribution mode ($\Delta d = d_{\mathrm{dilution}} - d_{\mathrm{no\_dilution}}$) increases from 520 to 1130 nm. It is important to point out that the alternative scheme was not used here and multiply charged particles are in this case the result of the coagulation of the small charged silver particles of the same charge polarity before they were grown larger. This coagulation process is quite normal at the high particle

concentrations used. However, as before, the peaks of multiply charged particles are not seen without adding dilution.

Conclusions

According to the analysis using the visual detection method, electric wind proved to be promoted by the increase of the electric field strength, the aerosol layer thickness and total particle concentration. Due to the limitations of this method, the effect of particle size on the formation of electric wind was not clear at first. However, investigation of the measured size spectra showed that the increase of particle size results in more extensive distortions indicating that the size of the particles also promotes the formation of electric wind.

The comparison of the measured size spectra revealed that when electric wind is promoted by the chosen conditions (particle concentration, size and charge distribution) then the width parameter of the size distribution increases, the mode of the size distribution is shifted to smaller diameters and the peaks of the multiply charged particles are smoothed out.

The distortion of the size distribution was seen in the VLDMA and Long-DMA measurement results, suggesting that electric wind should be taken into account in aerosol measurements and other applications of commercial DMAs when measuring large particles at high concentrations.

Acknowledgements: This work was supported by institutional research funding IUT20-11 of the Estonian Ministry of Education and Research.

References

Bondar H. & Bastien F. 1986. Effect of neutral fluid velocity on direct conversion from electrical to fluid kinetic energy in an electro-fluid-dynamics (EFD) device. *Journal of Physics D* 19: 1657–1663.

Chow J.C., Watson J.G., Mauderly J.L., Costa D.L., Wyzga R.E., Vedal S., Hidy G.M., Altshuler S.L., Marrack D., Heuss J.M., Wolff G.T., Arden Pope C.III & Dockery D.W. 2006. Health effects of fine particulate air pollution: lines that connect. *Journal of the Air & Waste Management Association* 56: 1368–1380.

Flagan R.C. 1998. History of electrical aerosol measurements. *Aerosol Science and Technology* 28: 301–380.

Fuchs N.A. 1963. On the stationary charge distribution on aerosol particles in a bipolar ionic atmosphere. *Geofisica pura e applicata* 56: 185–193.

Harney D.S. 1957. *An aerodynamic study of the "electric wind"*. Engineer's thesis, California Institute of Technology.

Hawley R. 1965. Electrical coronas. *Electronics & Power* 11: 388–393.

Hinds W.C. 1999. *Aerosol technology: properties, behavior, and measurement of airborne particles*. John Wiley and Sons Inc., New York.

Hoppel W.A. 1978. Determination of the aerosol size distribution from the mobility distribution of the charged fraction of aerosols. *Journal of Aerosol Science* 9: 41–54.

Knutson E.O. & Whitby K.T. 1975. Accurate measurement of aerosol electric mobility moments. *Journal of Aerosol Science* 6: 453–460.

Ku B.K., Maynard A.D., Baron P.A. & Deye G.J. 2007. Observation and measurement of anomalous responses in a differential mobility analyzer caused by ultrafine fibrous carbon aerosols. *Journal of Electrostatics* 65: 542–548.

Liu B.Y.H. & Pui D.Y.H. 1974. A submicron aerosol standard and the primary, absolute calibration of the condensation nuclei counter. *Journal of Colloid and Interface Science* 47: 155–171.

Peil I. & Tamm E. [Пеил И. & Тамм Е.] 1984. [Generation of monodisperse aerosols by the electrostatic separation method]. *Acta et Commentationes Universitatis Tartuensis* 669: 38–52. [In Russian with English summary].

Robinson M. 1960. *Movement of air in the electric wind of the corona discharge*. Research-Cottrell, Inc., Bound Brook, New Jersey.

Robinson M. 1962. A history of the electric wind. *American Journal of Physics* 30: 366.

Seinfeld J.H. & Pandis S.N. 2006. *Atmospheric chemistry and physics: from air pollution to climate change*. John Wiley and Sons Inc., New York.

Uin J. & Tamm E. 2010. Assessment of the quality of electrically produced standard aerosols. *Aerosol and Air Quality Research* 10: 609–615.

Uin J., Tamm E. & Mirme A. 2009. Electrically produced standard aerosols in a wide size range. *Aerosol Science and Technology* 43: 847–853.

Uin J., Tamm E. & Mirme A. 2011. Very long DMA for the generation of the calibration aerosols in particle diameter range up to 10 μm by electrical separation. *Aerosol and Air Quality Research* 11: 531–538.

Wang S.C. & Flagan R.C. 1990. Scanning electrical mobility spectrometer. *Aerosol Science and Technology* 13: 230–240.

Wiedensohler A. 1988. An approximation of the bipolar charge distribution for particles in the submicron size range. *Journal of Aerosol Science* 19: 387–389.